Electronic and Geometric Structure of Bimetallic Clusters: Density Functional Calculations on $[M_4\{Fe(CO)_4\}_4]^{4-}$ (M = Cu, Ag, Au) and $[Ag_{13}\{Fe(CO)_4\}_8]^{n-}$ (n = 0−5)

Katrin Albert,[†] Konstantin M. Neyman,[†] Gianfranco Pacchioni,[‡] and Notker Rösch*[,†]

Lehrstuhl für Theoretische Chemie, Technische Universität München, D-85747 Garching, Germany, and Dipartimento di Chimica Inorganica, Metallorganica e Analitica, Università di Milano, via Venezian 21, I-20133 Milan, Italy

Received March 13, 1996[⊗]

The results of all-electron density functional calculations on the bimetallic cluster compounds $[M_4\{Fe(CO)_4\}_4]^{4-}$ (M = Cu, Ag, Au) and on the corresponding naked species M_4Fe_4 are reported. The trends within the triad have been investigated. The bare metal clusters exhibit a strong magnetization which is quenched on addition of CO ligands. The bonding in the bare clusters is different for the silver derivative compared to that of copper and gold, resulting in comparatively weaker Ag−Fe and Ag−Ag bonds. This can be rationalized in terms of the different d−sp mixing, which for Cu and Au is larger than for Ag. Relativistic effects act to increase the 4d−5s mixing in Ag and to strengthen the intermetallic bond with Fe. In the carbonylated clusters a charge transfer from the metal M (M = Cu, Ag, or Au) to the $Fe(CO)_4$ groups occurs so that the atoms M can be considered in a formal +I oxidation state, rationalizing the nearly square-planar geometry of the metal frame. In fact, the local coordination of the M atoms is almost linear, as expected for complexes of M(I). The addition of extra electrons results in a stabilization of the clusters, indicating the electron-deficient nature of these compounds. Similar features have been found for the largest cluster synthesized so far for this class of compounds, $[Ag_{13}\{Fe(CO)_4\}_8]^{n-}$, ($n$ = 0−5). The nature and localization of the unpaired electron in the tetraanion is also discussed.

1. Introduction

Bimetallic cluster compounds containing a group 11 element stabilized by peripheral $Fe(CO)_4$ groups show an interesting structural variety. Clusters of the composition $[M\{Fe(CO)_4\}_2]^{3-}$ (M = Ag, Au),[1,2] $[Cu_3\{Fe(CO)_4\}_3]^{3-}$,[3] $[M_4\{Fe(CO)_4\}_4]^{4-}$ (M = Ag, Au),[1,2] $[M_5\{Fe(CO)_4\}_4]^{3-}$ (M = Cu, Ag),[1,3] $[M_6\{Fe(CO)_4\}_3]^{2-}$ (M = Cu, Ag),[4,5] and $[Ag_{13}\{Fe(CO)_4\}_8]^{n-}$ (n = 3, 4, 5)[6,7] have been synthesized. The metal core of compounds containing up to five coinage metal atoms is planar, while the larger moieties adopt an idealized tetrahedral or octahedral geometry. The clusters of different stoichiometry interconvert readily in solution.[3,7] The $Fe(CO)_4$ groups act as μ_2- or μ_3-ligands which formally correspond to two or four electron donors, respectively. However, because of the presence of low-lying empty levels, they can also act as Lewis acids, taking up two electrons. The $Fe(CO)_4$ fragment has been the subject of many theoretical investigations, and its orbital structure is well-understood.[1,8,9] There has been an intensive discussion about the bonding in the title compounds.[1,6,7] In particular, the question has been raised if M−M bonding is present and why some clusters are not formed by one element although they can be synthesized with the other two members of the triad. One example of this behavior is the formation of a trimer of $[M\{Fe(CO)_4\}]^-$ in the case of copper while silver and gold form a tetrameric structure.[1,3] There have been attempts to rationalize the electronic structure of $[Ag_4\{Fe(CO)_4\}_4]^{4-}$ with the help of extended-Hückel calculations.[1] A series of carbonylated bimetallic clusters containing copper has been investigated with the Fenske−Hall method.[10]

In this paper we report the results of all-electron density functional studies on the $[M_4\{Fe(CO)_4\}_4]^{4-}$ clusters with M = Cu, Ag, Au as well as on the bare ("naked") clusters of the type M_4Fe_4. The main goal is to explore the periodic trends in the group and the importance of relativistic effects for M = Ag. (Only the silver compounds are calculated both nonrelativistically and relativistically since it is well-known that relativistic effects are of no importance for 3d metals and indispensable for a correct description of 5d metals.[11]) Such an investigation allows one to gain insight into the geometric and electronic structure of these compounds. It will be shown that there exist considerable differences in the bonding mechanisms and that in all three cases M−M bonding is present. We also investigated the largest cluster in this series synthesized so far, namely, $[Ag_{13}\{Fe(CO)_4\}_8]^{n-}$, n = 0−5. The fragmentation energies have been determined as a function of the cluster charge; the nature and localization of the unpaired electron in $[Ag_{13}\{Fe(CO)_4\}_8]^{4-}$ has also been considered.

The present investigation of bimetallic carbonyl cluster compounds lies at the intersection of two avenues of cluster

* Author to whom correspondence should be addressed.
[†] Technische Universität München.
[‡] Università di Milano.
[⊗] Abstract published in *Advance ACS Abstracts,* November 15, 1996.

(1) Albano, V. G.; Azzaroni, F.; Iapalucci, M. C.; Longoni, G.; Monari, M.; Mulley, S.; Proserpio, D. M.; Sironi, A. *Inorg. Chem.* **1994**, *33*, 5320.
(2) Albano, V. G.; Calderoni, F.; Iapalucci, M. C.; Longoni, G.; Monari, M. *J. Chem. Soc., Chem. Commun.* **1995**, 433.
(3) Doyle, G.; Eriksen, K. A.; Engen, D. V. *J. Am. Chem. Soc.* **1986**, *108*, 445.
(4) Doyle, G.; Eriksen, K. A.; Engen, D. V. *J. Am. Chem. Soc.* **1985**, *107*, 7914.
(5) Briant, C. E.; Smith, R. G.; Mingos, D. M. P. *J. Chem. Soc., Chem. Commun.* **1984**, 586.
(6) Albano, V. G.; Grossi, L.; Longoni, G.; Monari, M.; Mulley, S.; Sironi, A. *J. Am. Chem. Soc.* **1992**, *114*, 5708.
(7) Albano, V. G.; Azzaroni, F.; Iapalucci, M. C.; Longoni, G.; Monari, M.; Mulley, S. In *Chemical Processes in Inorganic Materials: Metal and Semiconductor Clusters and Colloids*; Persans, P. D., Bradley, J. S., Chianelli, R. R., Schmidt, G., Eds.; Symposium Proceedings; Materials Research Society: Pittsburgh, PA, 1992; Vol. 272.
(8) Elian, M.; Hoffmann, R. *Inorg. Chem.* **1975**, *14*, 1058.
(9) Daniel, C.; Bénard, M.; Dedieu, A.; Wiest, R.; Veillard, A. *J. Phys. Chem.* **1984**, *88*, 4805.
(10) Buhl, M. L.; Long, G. J.; Doyle, G. *J. Organomet. Chem.* **1993**, *461*, 187.
(11) Pyykkö, P. *Chem. Rev.* **1988**, *88*, 563.

S0020-1669(96)00274-1 CCC: $12.00

chemistry that have previously been pursued by us, those toward an understanding of the electronic structure of transition metal carbonyl clusters[12,13] and of "naked" bimetallic clusters.[14,15]

2. Computational Details

The "first principles" linear combination of Gaussian-type orbitals density functional (LCGTO-DF) method[16] used in the present study allows one to perform all-electron self-consistent field (SCF) density functional calculations. The local density approximation (LDA) suggested by Vosko, Wilk, and Nusair[17] was used in the geometry optimizations. For the geometries thus obtained, gradient corrections to the exchange[18] and to the correlation[19] energy functional were computed self-consistently (nonlocal density approximation, NLDA) to determine the binding energies more accurately as the LDA approach tends to overestimate binding energies.[20] A scalar-relativistic variant of the LCGTO-DF method, implemented in a self-consistent fashion, has been applied in the calculations of the clusters containing gold atoms.[21,22] The fractional occupation numbers (FON) approach was used to determine the orbital occupancies.[16] According to this procedure, each one-electron level is broadened by a Gaussian (0.3 eV half-width) and the resulting "bands" are filled up to the cluster Fermi energy, ϵ_F, which is thus computed in a self-consistent way. This FON approach has the special merit in that, besides accelerating the SCF convergence, it bypasses the problem associated with an investigation of several close-lying configurations. Spin unrestricted calculations were performed whenever ground states of the compounds considered correspond to open-shell electronic configurations. Atomic charges were computed with the help of a Mulliken population analysis.

The orbital basis sets for C and O from ref 23 were augmented by one d exponent as described previously.[24] The construction of the Fe and Cu orbital basis sets started from the (14s9p5d) ones,[25] which were improved[26] by adding one s and two diffuse p exponents; one additional d exponent was taken from ref 27. The Ag basis set, originally from ref 28, was modified as previously described.[29] The basis set for Au was also taken as in previous DF studies.[30] The final basis sets were contracted in a generalized fashion using LDA atomic eigenvectors: C, O, (9s5p1d) → [5s4p1d]; Fe, Cu, (15s11p6d) → [6s5p3d]; Ag, (18s13p8d) → [8s6p4d]; Au, (19s15p10d6f) → [9s8p5d2f]. Two different sets of orbital contractions were employed for Fe and Ag in the relativistic and in the nonrelativistic calculations. The auxiliary basis sets used in the LCGTO-DF method to represent the electron charge density and the exchange-correlation potential were constructed from the orbital exponents in a standard fashion.[16]

The geometries of Cu and Ag containing clusters were optimized using analytical energy gradients[31−33] of the nonrelativistic LDA total energy and a variable metric update scheme based on internal coordinates[34] to locate the minimum of the potential energy surface. The Ag containing species were recalculated at the relativistic level without geometry change. For the relativistic calculation of the Au_4Fe_4 cluster, a cyclic optimization of all degrees of freedom that are allowed by the D_{4h} symmetry constraint was employed. The search was stopped after all of the varied interatomic distances changed by less than 0.001 Å.

Geometry optimization of the clusters containing four coinage metal atoms was carried out in D_{4h} symmetry; the fragment $Fe(CO)_4$ was optimized in C_{2v} symmetry. The cluster $[Au_4\{Fe(CO)_4\}_4]^{4-}$ was calculated in D_{4h} symmetry with averaged bond lengths and angles taken from the crystal structure.[2] For the cluster $[Ag_{13}\{Fe(CO)_4\}_8]^{n-}$, the averaged experimental geometry (O_h symmetry) was taken.[6] All Fe−C−O angles were fixed at 180°.

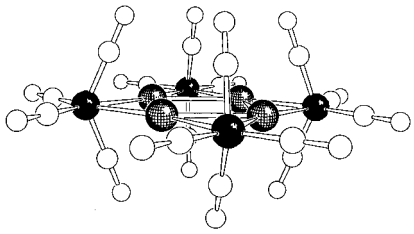

Figure 1. SCHAKAL[35] sketch of the optimized geometry of $[Ag_4\{Fe(CO)_4\}_4]^{4-}$: silver atoms, shaded; iron atoms, black.

Table 1. Interatomic Distances (Å) and Angles (deg) of $[M_4\{Fe(CO)_4\}_4]^{4-}$ Clusters (M = Cu, Ag, Au) and of the $Fe(CO)_4$ Molecule

	Cu	Ag		Au	$Fe(CO)_4$
geometric param	*a*	*a*	*b*	*b*	*a*
M−M	2.56	2.96	3.15	2.90	
M−Fe	2.38	2.60	2.58	2.61	
$Fe-C_{eq}$	1.73	1.73	1.75	1.75	1.77
$C_{eq}-O_{eq}$	1.18	1.18	1.16	1.15	1.15
$Fe-C_{ax}$	1.76	1.77	1.77	1.76	1.80
$C_{ax}-O_{ax}$	1.18	1.18	1.17	1.15	1.15
$\angle C_{eq}-Fe-C_{eq}$	106.5	106.4	103.0	106.0	97.5
$\angle C_{ax}-Fe-C_{ax}$	131.3	135.7	135.4	148.0	150.8
∠Fe−Me−Fe	155.1	159.4	165.4	157.4	

[a] Calculated Geometries. [b] Geometries based on averaged experimental values.[1,2]

3. Results and Discussion for Clusters with the M_4Fe_4 Skeleton

3.1. Cluster Geometries. The optimized structure of the anion $[M_4\{Fe(CO)_4\}_4]^{4-}$ is exemplified in Figure 1 for M = Ag. The cluster contains an idealized square of M atoms surrounded by four μ_2-bridging $Fe(CO)_4$ groups. Two CO ligands of a $Fe(CO)_4$ moiety lie in the plane of the metal core (and will be referred to as equatorial); the other two are in vertical planes (axial). This compound has been synthesized and structurally characterized for M = Ag and Au.[1,2]

The geometries of the bare and carbonylated cluster compounds are displayed in Table 1 together with the structure of a free $Fe(CO)_4$. The geometry of the $Fe(CO)_4$ moiety is similar in all three compounds except for the $C_{ax}-Fe-C_{ax}$ angle which increases in going from Cu to Au. The bending of the axial CO ligands is proposed to decrease with increasing electronegativity (EN) of M.[1] The Pauling EN values are as follows: Cu, 1.90; Ag, 1.93; Au, 2.54.[36] Accordingly, the bending angles in the cases of Cu and Ag are similar and smaller than that of

(12) Rösch, N.; Ackermann, L.; Pacchioni, G. *J. Am. Chem. Soc.* **1992**, *114*, 3549.
(13) Pacchioni, G.; Rösch, N. *Acc. Chem. Res.* **1995**, *28*, 390.
(14) Albert, K.; Neyman, K. M.; Nasluzov, V. A.; Ruzankin, S. P.; Yeretzian, C.; Rösch, N. *Chem. Phys. Lett.* **1995**, *245*, 671.
(15) Heiz, U.; Vayloyan, A.; Schumacher, E.; Yeretzian, C.; Stener, M.; Rösch, N. *J. Chem. Phys.*, in press.
(16) Dunlap. B. I.; Rösch, N. *Adv. Quantum Chem.* **1990**, *21*, 317.
(17) Vosko, S. H.; Wilk, L.; Nusair, M. *Can. J. Phys.* **1980**, *58*, 1200.
(18) Becke, A. D. *Phys. Rev. A* **1988**, *38*, 3098.
(19) Perdew, J. P. *Phys. Rev. B* **1986**, *33*, 8822.
(20) Ziegler, T. *Chem. Rev.* **1991**, *91*, 651.
(21) Häberlen, O. D.; Rösch, N. *Chem. Phys. Lett.* **1992**, *199*, 491.
(22) Rösch, N.; Krüger, S.; Mayer, M.; Nasluzov, V. In *Recent Developments and Applications of Modern Density Functional Theory*; Seminario, J. M., Ed.; Elsevier: Amsterdam, 1996; p 497.
(23) van Duijneveldt, F. B. IBM Research Report No. RJ 945 1971.
(24) Neyman, K. M.; Ruzankin, S. P.; Rösch, N. *Chem. Phys. Lett.* **1995**, *246*, 546.
(25) Wachters, A. J. H. *J. Chem. Phys.* **1970**, *52*, 1033.
(26) Ulbricht, P.; Häberlen, O.; Weinelt, M.; Steinrück, H.-P.; Rösch, N. *Surf. Sci.* **1995**, *326*, 53.
(27) Hay, P. J. *J. Chem. Phys.* **1977**, *66*, 4377.
(28) Huzinaga, S. *J. Chem. Phys.* **1977**, *66*, 4245.
(29) Neyman, K. M.; Rösch, N. *Surf. Sci.* **1993**, *287*, 64.
(30) Häberlen, O. D.; Chung, S.-C.; Rösch, N. *Int. J. Quantum Chem.: Quantum Chem. Symp.* **1994**, *28*, 595.
(31) Dunlap, B. I.; Andzelm, J.; Mintmire, J. W. *Phys. Rev. A* **1990**, *42*, 6354.
(32) Andzelm, J.; Wimmer, E. *J. Chem. Phys.* **1992**, *96*, 1280.
(33) Nasluzov, V. A.; Rösch, N. *Chem. Phys.* **1996**, *210*, 413.
(34) Gill, P. E.; Murray, W.; Wright, M. H. *Practical Optimization*; Academic Press: London, 1981.
(35) Keller, E. *SCHAKAL92*; Kristallographisches Institut der Universität Freiburg: Freiburg, Germany, 1992.

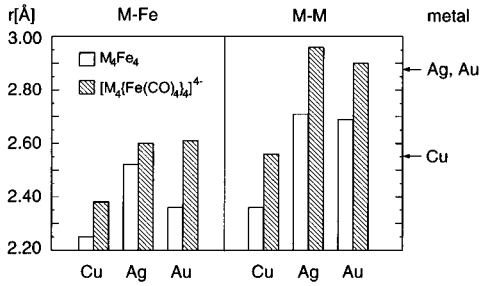

Figure 2. M−Fe and M−M bond lengths of naked and ligated clusters. The corresponding M−M distance in the bulk metal is indicated by an arrow on the right.

the Au derivative, where the $C_{ax}-Fe-C_{ax}$ angle is close to the value in the free $Fe(CO)_4$ molecule. The angles between the equatorial ligands clearly show no such dependence on the type of metal atom M. In the free $Fe(CO)_4$ molecule the angle $C_{ax}-Fe-C_{ax}$ decreases with increasing negative molecular charge[8,37] in line with our calculated values: $Fe(CO)_4$, 150.8°; $Fe(CO)_4^-$, 131.5°; $Fe(CO)_4^{2-}$, 109.8°. Thus, the total electron density on the $Fe(CO)_4$ moiety bound to an electronegative atom should be lower than in the case of a less electronegative atom. Consequently, the angle $C_{ax}-Fe-C_{ax}$ is expected to be larger in the latter complex.

The only significant difference between the averaged experimental and the optimized geometry of the Ag cluster is the Ag−Ag bond length which is calculated to be 0.2 Å shorter. In the crystal structure this bond length ranges from 3.04 to 3.33 Å, while in other clusters there are considerably shorter Ag−Ag contacts, for example, 2.80 Å in $[Ag_5\{Fe(CO)_4\}_4]^{3-}$.[1] This fluctuation of Ag−Ag separations prompted us to investigate the energy changes upon an elongation of this bond distance, keeping the position of the other atoms fixed. As the calculated change in total energy is less than 0.1 eV in the range of 2.96 ± 0.2 Å, the discrepancy in the Ag−Ag distances should be attributed to the very soft Ag−Ag breathing mode in $[Ag_4\{Fe(CO)_4\}_4]^{4-}$. The softness of the M−M contacts has also been used as an explanation for the strong distortions of the Ag_4 unit in $[Ag_4\{Fe(CO)_4\}_4]^{4-}$.[2]

The geometry of the bare M_4Fe_4 has been optimized to elucidate the influence of the CO ligands on the metal core. The resulting M−M and M−Fe bond lengths are displayed in Figure 2 together with the corresponding values in the carbonylated clusters and the distance in the bulk metal. The distances exhibit the characteristic trend also found in other compounds of group 11 elements:[38] the bond lengths in the Ag clusters are longer than in the Cu clusters and similar or even longer than in the Au congeners. This finding is explained by relativistic effects, which lead to a stabilization of the 6s orbital and a destabilization of the 5d orbitals, thus favoring sd mixing.[11] The M−M bond lengths may be rationalized as follows: the M s valence orbitals in a square-planar arrangement result in a bonding a_{1g}, a nonbonding e_u, and an antibonding b_{2g} level. In the naked clusters these levels lie below (a_{1g}, e_u) or at the Fermi level (b_{2g}). Due to the interaction with the CO ligands, the levels are pushed above the Fermi level, so that the M−M bonds are weakened and the distances are longer than the corresponding value in the bulk metal. Nevertheless, there remains M−M bonding, and the departure from the linear Fe−M−Fe arrangement may be regarded as a measure of the strength of the M−M interactions.[1] The Fe−M−Fe angles (Table 1) decrease along the series Ag > Au > Cu. The M−Fe bonding differs substantially in the three clusters due to a different amount of the d−d overlap. In Cu_4Fe_4 and Au_4Fe_4 clusters the Cu and Au d manifold is energetically close to the Fe 3d orbitals so that some mixing is possible; in Ag_4Fe_4, on the other hand, the Fe 3d levels are well above the Ag 4d band, and almost no mixing occurs (see Figure 5). In this cluster only the s derived a_{1g} and e_u levels contribute to M−Fe bonding, increasing the bond distance in Ag_4Fe_4 (Figure 2). In the carbonylated clusters the M−Fe distance is longer than the sum of covalent radii (Fe, Cu, 1.17 Å; Ag, Au, 1.34 Å)[36] due to a destabilization of the M and Fe s orbitals caused by their interaction with the CO ligands.

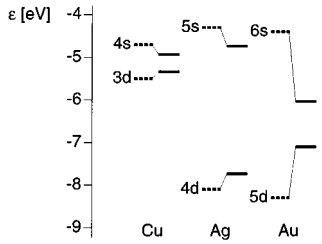

Figure 3. One-electron energy levels of the copper triad from a nonrelativistic (- -) and a relativistic (—) calculation of the $d^{10}s^1$ ground state. The spin−orbit interaction has not been taken into account.

Table 2. Fragmentation Energies[a] ΔE (eV) of Naked and Carbonylated M_4Fe_4 Clusters (M = Cu, Ag, Au) Calculated at the Nonrelativistic (nrel) and Relativistic (rel) Levels of Theory

	Cu	Ag		Au
cluster	nrel	nrel	rel	rel
M_4Fe_4	15.8	12.0	13.2	15.8
$M_4\{Fe(CO)_4\}_4$	44.3	41.7	43.0	45.2
$[M_4\{Fe(CO)_4\}_4]^{4-}$	43.8	42.6	44.4	43.1

[a] $\Delta E = E(M_4Fe_4CO_n) - 4E(M) - 4E(Fe) - nE(CO)$.

3.2. Binding Energies. The fragmentation energy, i.e., the energy needed to separate the cluster into M and Fe atoms and CO molecules, is shown in Table 2 for the naked and carbonylated clusters. The orbital diagrams for the atoms Cu, Ag, and Au (Figure 3) are helpful in understanding differences in the fragmentation energies. The nonrelativistic s−d separation increases from Cu to Au. Relativistic effects lead to a contraction and energetic lowering of the valence s orbital, while the d orbitals are destabilized and become more diffuse. As expected, in Cu and Ag, the relativistic effect is small, whereas, in Au, the s orbital is lowered by more than 2 eV. As a result, in Cu and Au the s and d levels lie close, while in Ag they are well-separated.

For the bare clusters Cu_4Fe_4 and Au_4Fe_4 the binding energies are equal and 3.8 eV larger than that for Ag_4Fe_4. This indicates that the s−d hybridization plays an important role in the bonding. The weaker Ag−Fe bond is reflected by a comparatively long Ag−Fe bond distance (section 3.1). In order to quantify the strength of the M−M bonds in the M_4Fe_4 compounds, the atomization energies of the M_4 subunits have been calculated. The Ag−Ag bond is weaker than the Cu−Cu and Au−Au bonds, which is reflected by the corresponding atomization energies: 4.0, 5.2, and 5.4 eV, respectively. The atomization energy of Ag_4Fe_4 increases by 1.2 eV due to relativistic effects. It has been shown for diatomics AuX that both a stabilization and a destabilization due to relativistic effects is possible, depending on the EN of the ligand X.[38] A relativistic stabilization is expected for EN(X) < EN(Au). The present results suggest a similar relationship for Ag compounds, EN-

(36) Varga, T. K., Bello, C., Eds. *Periodic Table of the Elements*; Papertech Marketing Group, Inc.: Concord, Ontario, Canada, 1994.
(37) Albright, T. A.; Burdett, J. K.; Whangbo, M.-H. *Orbital Interactions in Chemistry*; Wiley: New York, 1985.
(38) Schwerdtfeger, P.; Dolg, M.; Schwarz, W. H. E.; Bowmaker, G. A.; Boyd, P. D. W. *J. Chem. Phys.* **1989**, *91*, 1762.

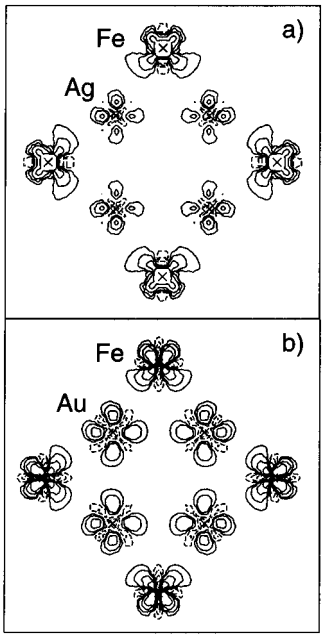

Figure 4. Difference density $\Delta\rho = \rho([M_4\{Fe(CO)_4\}_4]^{4-}) - \rho(M_4\{Fe(CO)_4\}_4)$ in the plane containing all metal atoms. Only the metal cores of the clusters are shown. (a) M = Ag; (b) M = Au. The contour lines correspond to values of 0.004, 0.01, 0.025, and 0.063 au.

(Fe) = 1.83, EN(Ag) = 1.93. As pointed out in section 3.1, in the nonrelativistic case the Ag d band lies below the Fe d band. The relativistic destabilization of the Ag d orbitals results in some Ag d/Fe d mixing and a strengthening of the Ag−Fe bond.

For the neutral $M_4\{Fe(CO)_4\}_4$ clusters, the Au compound is about 1 eV more stable than the Cu analogue; the Ag cluster again exhibits the lowest stability. The relativistic stabilization of the Ag compound is similar to that in the naked cluster. The addition of four electrons (resulting in the experimentally characterized tetraanion) stabilizes the Ag compound by 0.9 eV in the nonrelativistic calculation and by 1.4 eV in the relativistic case, whereas the Cu and Au clusters are destabilized by 0.5 and 2.1 eV, respectively (Table 2). As can be seen from Figure 4, the change in the binding energy on addition of the four electrons correlates with the electron density increase on the M atoms: the silver cluster (Figure 4a), stabilized with respect to the neutral compound, exhibits the smallest density increase, while the gold (Figure 4b) and copper (not shown) analogues, which are destabilized, show a larger electron density gain. While the clusters with a 4-fold negative charge are less stable than the neutral ones for M = Cu and Au, the addition of two electrons leads to a considerable stabilization of all compounds. The calculated double electron affinities for the copper, silver, and gold clusters are 7.0, 7.0, and 6.0 eV, respectively.

3.3. Density of States. Spin polarization leads to a preferred occupation of one-electron states corresponding to one of the two possible spin directions, which are called majority and minority spin states, respectively. In the density of states (DOS) of the M_4Fe_4 clusters the minority and majority spin components are displayed separately (Figure 5), the latter ones being completely filled, while the former ones are only partially filled, resulting in a net magnetization of all systems with approximately 13 unpaired eletrons. As mentioned before, these plots show that the majority spin Fe d orbitals overlap with Cu and Au d orbitals, but are energetically separated from the Ag d orbitals in the Ag cluster. Due to this interaction the Cu and Au d bands spread over a wider energy range than that of the Ag d band. A detailed analysis shows that the Ag contribution to the Fe d band stems from the s derived e_u orbital. As the

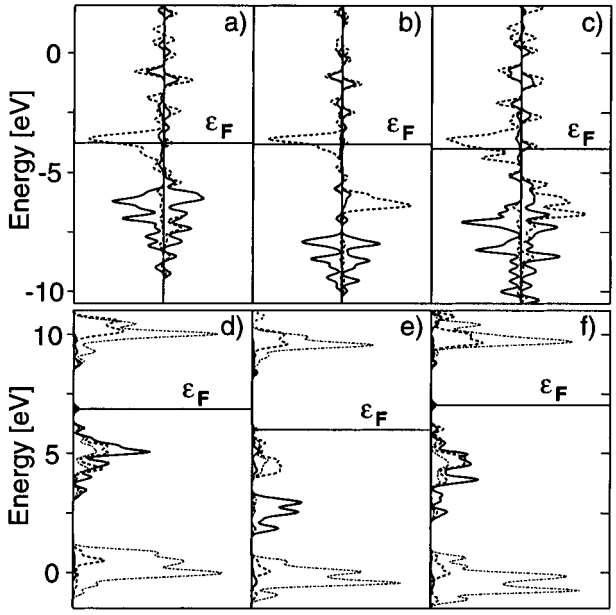

Figure 5. Density of states (DOS, in arbitrary units) of the optimized clusters M_4Fe_4 (a−c) and the $[M_4\{Fe(CO)_4\}_4]^{4-}$ (d−f), generated by Gaussian broadening (0.1 eV) of the one-electron energy spectrum: (a, d) M = Cu; (b, e) M = Ag; (c, f) M = Au; (—) contribution from M, (- -) contribution from Fe, (— · —) contribution from CO; (a−c) left side minority spin, right side majority spin. ϵ_F indicates the Fermi level.

DOS plot of the relativistic Ag_4Fe_4 does not differ much from the nonrelativistic one (the Ag d band is 0.5 eV higher in energy), we refrain from showing it. The calculated Fermi energy is similar for all three bare M_4Fe_4 clusters (see Figure 5a−c).

The interaction with the CO ligands changes the orbital structure drastically, Figure 5d,e. The carbonylated anionic clusters are closed-shell systems with a large HOMO−LUMO gap. As a consequence of the spin pairing the magnetization of the naked clusters is quenched. Similar effects have been observed for carbonylated Ni clusters.[13] The Fermi energy of the Ag cluster is lowered with respect to the other two, and the d bands are narrower in comparison with the naked clusters. The effect of the CO ligands on the electronic configuration will be discussed below.

3.4. Atomic Charges and Electron Configuration. The analysis of the electron configuration of the cluster compounds and of the charge on the atoms M helps to further understand the bonding mechanism (Table 3). As mentioned in section 3.1, the M−M bonding in the naked clusters is governed by the four s derived orbitals a_{1g}, e_u, and b_{2g}. (Recall the relative energy of the s and d orbitals in Cu, Ag, and Au from Figure 3). The energy splitting of the diffuse s orbitals is larger than that of the more localized d orbitals. The level ordering in a M_4 subunit is thus different for the three members of the triad: in Ag_4, the s derived levels lie above the d levels, while in Cu_4 and Au_4 the a_{1g} orbital is at the bottom of the d band. The Au 6s atomic orbital (AO) is deepest in energy in the triad; thus, Au_4Fe_4 has the largest s population and, correspondingly, a slightly negative atomic charge on Au (Table 3). In Cu_4Fe_4 the s derived orbitals lie at lower energies in comparison to Ag_4Fe_4, while the d band is situated higher but spreads over a wider energy range due to the interaction with the Fe d band (Figure 5). Accordingly, the Ag s orbital is less populated and Ag has a slightly larger positive atomic charge than Cu. The d and p populations on Fe do not differ significantly in all three naked clusters. The Fe s derived orbitals interact mainly with s orbitals of M. The M s population decreases in the order Au

Table 3. Mulliken Populations and Atomic Charges *q* (au) of Naked and Carbonylated Clusters, Calculated at the Nonrelativistic (nrel) and Relativistic (rel) Levels of Theory

		M				Fe			
system		s	p	d	q	s	p	d	q
Cu_4Fe_4	nrel	1.00	0.38	9.61	0.01	1.11	0.15	6.75	−0.01
Ag_4Fe_4	nrel	0.86	0.36	9.69	0.10	1.19	0.16	6.74	−0.10
Ag_4Fe_4	rel	0.93	0.37	9.63	0.07	1.19	0.19	6.69	−0.07
Au_4Fe_4	rel	1.20	0.39	9.49	−0.11	1.02	0.22	6.65	0.11
$[Cu_4\{Fe(CO)_4\}_4]^{4-}$	nrel	0.77	0.19	9.69	0.35	0.44	1.04	7.00	−0.48
$[Ag_4\{Fe(CO)_4\}_4]^{4-}$	nrel	0.63	0.17	9.70	0.50	0.39	1.22	7.06	−0.66
$[Ag_4\{Fe(CO)_4\}_4]^{4-}$	rel	0.72	0.18	9.66	0.44	0.40	1.25	7.02	−0.67
$[Au_4\{Fe(CO)_4\}_4]^{4-}$	rel	0.91	0.22	9.63	0.22	0.48	1.14	7.04	−0.66

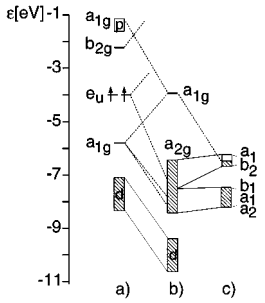

Figure 6. Orbital interaction diagram between Ag_4 (a) and $[Fe(CO)_4]_4$ (c) (orbital notation for one $Fe(CO)_4$ unit) to yield the $[Ag_4\{Fe(CO)_4\}_4]^{4-}$ cluster (b). The filled bands are shaded. The HOMO of each fragment is marked by the electrons residing in it.

> Cu > Ag and reflects the energetic position of the M s AO relative to the Fe s one (−5.4 eV).[37] The relativistic effect stabilizes the Ag s orbitals and destabilizes the Ag d band, leading to a slightly less positive charge on Ag. In the M_4Fe_4 clusters the configuration of iron changes from the atomic value of d^6s^2 to formally d^7s^1. In general, the intermetallic bond in the naked bimetallic clusters does not show an appreciable charge transfer. The situation is considerably different when the carbonylated clusters are considered.

The addition of CO ligands strongly affects the electronic structure of the bimetallic clusters in a way similar to that described for nickel carbonyls.[13] CO molecules induce a noticeable charge transfer from M to Fe which decreases along the series Ag > Cu > Au. This charge redistribution can be considered as a change of the formal oxidation state of M from 0 to +I, important for rationalizing the cluster geometries. In fact, Cu(I), Ag(I), and Au(I) compounds show a general tendency to form linear complexes of the type X−M−X (X = Cl^-, NH_3, etc.).[39] This is the same arrangement assumed by the Cu, Ag, and Au atoms in the tetrameric carbonylated clusters and, with some minor distortion, also by the Ag atoms in the compact $[Ag_{13}(Fe(CO)_4)_8]^{n-}$ cluster.

3.5. Orbital Analysis. Another approach to analyze the electronic structure of the title compounds is to investigate their orbitals by constructing an orbital correlation diagram from two subunits whose orbital structure is relatively simple. As usual, the region around the Fermi level is of interest. Since the MOs in this region have mostly Fe and M contributions (Figure 5d−f), it is convenient to split the cluster into a M_4 fragment and four $Fe(CO)_4$ moieties and to carry out the analysis in terms of fragment orbitals.

M_4 (Figure 6a). The orbital structure of the M_4 subunit in the geometry of the carbonylated cluster is exemplified for Ag_4 in Figure 6a. The HOMO e_u is filled with two electrons. As the Au−Au distance is shorter than the Ag−Ag one and the Au d orbitals have a larger radial expectation value (0.86 compared to 0.74 Å for Ag), the d band of the Au_4 unit is broader than that of Ag_4. In Cu_4 both the bond length and the radial expectation value are smaller than in Ag_4, so that the d band has approximately the same width as that of Ag_4.

$Fe(CO)_4$ (Figure 6c). $Fe(CO)_4$ (C_{2v} geometry) has a triplet ground state and can be formally considered as a two-orbital−two-electron donor.[1] The two frontier orbitals shown in Figure 6c are a_1 and b_2 with Fe p and d character and some CO contribution. If four $Fe(CO)_4$ groups are assembled in D_{4h} geometry, the a_1 orbital splits into a_{1g}, e_u, and b_{1g} levels and the b_2 orbital splits into b_{2g}, e_u, and a_{2g} levels. Since the distance of the $Fe(CO)_4$ units in the full cluster is rather large, the splitting is small compared to that in the M_4 units. The resulting level ordering for the $[Fe(CO)_4]_4$ moiety with the geometry taken from $[Ag_4\{Fe(CO)_4\}_4]^{4-}$ is displayed in Figure 6c. The HOMO is the doubly occupied a_{1g} level. The MOs below these frontier orbitals exhibit Fe d and CO contributions.

$M_4\{Fe(CO)_4\}_4$ (Figure 6b). It is seen from the interaction scheme in Figure 6 that the Ag d orbitals are strongly stabilized by the interaction with the $Fe(CO)_4$ groups. This is a direct, observable consequence of the charge transfer from Ag to $Fe(CO)_4$. In fact, the rather localized d orbitals are quite sensitive to changes in the atomic charge. The upper band consists of Fe 3d−CO levels. The frontier orbitals of the $[Fe(CO)_4]_4$ fragment essentially maintain their character and are stabilized by the interaction with Ag_4, while the s derived MOs of the Ag_4 subunit are significantly destabilized. Four electrons from the latter orbitals are transferred into the orbitals of $[Fe(CO)_4]_4$, and thus Ag becomes formally Ag(I). Since in the synthesized cluster four additional electrons are present, finally all orbitals of the $[Fe(CO)_4]_4$ subunit are filled. The fact that a net charge transfer from Ag to $Fe(CO)_4$ takes place shows that the $Fe(CO)_4$ unit does not act as an electron donor, as is usually assumed in electron counting schemes, but rather as a Lewis acid.

The level ordering in the $[Cu_4\{Fe(CO)_4\}_4]^{4-}$ and $[Au_4\{Fe(CO)_4\}_4]^{4-}$ clusters remains essentially the same as that for the Ag analogue. However, they exhibit a larger degree of mixing between the orbitals of the fragments. The M d orbitals interact stronger with the frontier orbitals of the $[Fe(CO)_4]_4$ fragment so that the a_{2g} and e_u MOs at the Fermi level have a larger M d contribution.

A charge transfer can in principle be monitored by the shift of core levels.[40,41] A shift to higher binding energies can be expected when the atomic charge decreases. Due to Pauli repulsion, core levels are shifted to lower binding energies. In the neutral carbonylated clusters, the M 1s levels lie deeper than in the corresponding bare M_4 unit by 3.19, 2.74, and 1.56 eV for Cu, Ag, and Au, respectively. In all cases the shift in the direction expected for a positively charged system is consistent

(39) Cotton, F. A.; Wilkinson, G. *Advanced Inorganic Chemistry*, 4th ed.; Wiley: New York, 1980.

(40) Bagus, P. S.; Brundle, C. R.; Pacchioni, G.; Parmigiani, F. *Surf. Sci. Rep.* **1993**, *19*, 265.

(41) Ågren, H. *Int. J. Quantum Chem.* **1991**, *39*, 455.

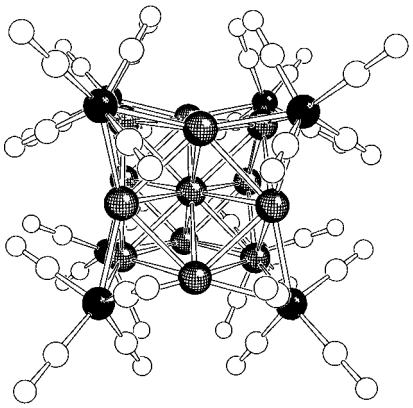

Figure 7. SCHAKAL[35] sketch of the averaged experimental geometry of the $[Ag_{13}\{Fe(CO)_4\}_8]^{4-}$ cluster anion: silver atoms, shaded; iron atoms, black.

with the shift of the valence orbitals and reinforces the view of the formal +I oxidation state of the M atoms in the carbonylated clusters. Unfortunately, a quantification of the charge on M is hardly possible because other terms contribute to the core level shifts, like the external electrostatic field, hybridization, and Pauli repulsion. The finding that the core levels of M in the M_4Fe_4 clusters lie below those of the bare M_4 units can be considered as an indication of a charge transfer from M to Fe in M_4Fe_4. However, the Mulliken net charge on M in the neutral M_4Fe_4 moieties is close to zero (Table 3), despite the rather large positive values calculated for the negatively charged carbonyl clusters.

4. Paramagnetic Anion $[Ag_{13}\{Fe(CO)_4\}_8]^{4-}$

The largest carbonylated Ag−Fe cluster which has so far been synthesized[6] is $[Ag_{13}\{Fe(CO)_4\}_8]^{4-}$ (Figure 7). The cluster core consists of 12 Ag atoms in a cuboctahedral arrangement with a central Ag atom. The averaged values of the center−surface Ag−Ag distances are the same as the Ag−Ag distances on the surface, 2.92 Å. Nevertheless, there is a significant dispersion in the Ag−Ag contacts (2.83−3.11 Å), and therefore the silver core is expected to be quite soft.[6] The $Fe(CO)_4$ groups are in this case μ_3-ligands (local symmetry C_{3v}) capping the triangular faces of the silver cluster. One CO group of $Fe(CO)_4$ is pointing radially away from the cluster; the other three lie approximately in one plane. It has been concluded from its ESR spectrum that the unpaired electron of the paramagnetic $[Ag_{13}\{Fe(CO)_4\}_8]^{4-}$ anion is partly localized on the central Ag atom. More precisely, the measured hyperfine coupling constants are consistent with a spin population of 0.25 on the central Ag and less than 0.01 on the orbitals of the peripheral Ag atoms.[6] Extended Hückel calculations support the interpretation of the ESR data.

An idealized experimental structure of $[Ag_{13}\{Fe(CO)_4\}_8]^{4-}$ in O_h symmetry has been employed in the present calculation. The bond distances are (in angstroms):[6] Ag−Ag, 2.92; Ag−Fe, 2.74; Fe−C_{ax}, 1.74; Fe−C_{eq}, 1.79; C_{ax}−O_{ax}, 1.16; C_{eq}−O_{eq}, 1.15. The bare metal cluster $Ag_{13}Fe_8$ was geometry optimized under O_h symmetry constraints which gave an Ag−Ag distance of 2.83 Å and an Ag−Fe distance of 2.55 Å.

The DOS of the bare cluster $Ag_{13}Fe_8$ (not shown) is similar to the Ag_4Fe_4 case: the Ag d band lies below the Fe d one; for iron, while the 3d majority spin component is completely filled, holes are present in the minority part, resulting in a net magnetization corresponding to 25 unpaired electrons in total or 3.1 unpaired electrons per iron atom, which agrees well with the value of 3.2 in the smaller Ag_4Fe_4 cluster. On addition of CO ligands, the magnetization is quenched and a HOMO−LUMO gap of about 1 eV is opened up.

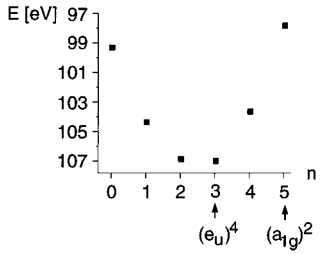

Figure 8. Fragmentation energies ΔE of $[Ag_{13}\{Fe(CO)_4\}_8]^{n-}$ for different n. $\Delta E = E([Ag_{13}\{Fe(CO)_4\}_8]^{n-}) - 13E(M) - 8E(Fe) - 32E(CO)$. Closed-shell configurations are marked by arrows.

As the anion $[Ag_{13}\{Fe(CO)_4\}_8]^{n-}$ has been shown to exist in solution for $n = 3-5$,[7] we calculated the fragmentation energies of the cluster for different values of n (Figure 8). The most stable cluster is found for $n = 3$ (binding energy, 106.9 eV), with $n = 2$ being only 0.1 eV less stable. This result can be explained by the MO structure of the cluster: in the neutral compound the HOMO is a singly occupied e_u level, which is filled with the extra electrons until for $n = 3$ a closed shell is reached. The next two electrons occupy the a_{1g} level. The neutral cluster has a positive electron affinity, and it can act as an electron reservoir; it is remarkable that the addition of two or three electrons leads to a large and virtually the same energy gain. $[Ag_{13}\{Fe(CO)_4\}_8]^{4-}$ is known to exist in the crystalline state. The free tetraanion is calculated to be only 2 eV less stable that the di- and trianions, an energy difference which can be gained through electrostatic interactions with the surrounding matrix omitted here. The central Ag atom acts to significantly stabilize the cluster, as the hypothetical anion $[Ag_{12}\{Fe(CO)_4\}_8]^{4-}$ without the central Ag atom, calculated in the geometry of $[Ag_{13}\{Fe(CO)_4\}_8]^{4-}$, is 2.65 eV less stable than the parent cluster.

Apparently, the occupation of the bonding e_u level leads to a stabilization of the cluster, while adding electrons in the antibonding a_{1g} level has a destabilizing effect. The discussion of the stability of a polynuclear cluster in terms of bonding, nonbonding, or antibonding characteristics of a single orbital, however, requires some care, given the highly delocalized nature of these systems. Nevertheless, an orbital analysis should help in characterizing the nature of the frontier e_u and a_{1g} orbitals. It is convenient to consider the interaction of the central silver atom with the Ag_{12} moiety first. On assembly of twelve Ag atoms in a cuboctahedral geometry, the valence s orbitals give a set of MOs a_{1g}, t_{1u}, t_{2g}, e_g, and t_{2u} in the sequence of increasing energy. The central Ag atom has one a_{1g} s orbital symmetry, so that the only bonding−antibonding combination of the fragment orbitals existing in the Ag_{13} cluster is the a_{1g} one (Figure 9a). The $Fe(CO)_4$ fragment in C_{3v} symmetry has two frontier orbitals, a filled e level and an empty a_1 level of Fe d−CO character. Below them is another orbital of e symmetry (Fe d). When eight $Fe(CO)_4$ groups are assembled in the geometry of the $[Ag_{13}\{Fe(CO)_4\}_8]^{4-}$ cluster compound, the a_1 levels split into a_{1g}, t_{1u}, t_{2g}, and a_{2u}, and the e levels split into e_g, t_{2u}, t_{1u}, t_{2g}, t_{1g}, and e_u. Again, the splitting is small due to the large distance between the $Fe(CO)_4$ groups (Figure 9c).

As in the case of $[Ag_4\{Fe(CO)_4\}_4]^{4-}$, the Ag d orbitals of Ag_{13} are strongly stabilized by the interaction with the $Fe(CO)_4$ groups (Figure 9). The orbitals derived from the two e levels of $Fe(CO)_4$ remain essentially unchanged, whereas two of the empty orbitals (a_{1g} and t_{1u}) are destabilized through the interaction with the orbitals of Ag_{13}. The other two empty orbitals are stabilized. Five electrons from the Ag_{13} subunit are filled into this band so that the HOMO in the neutral

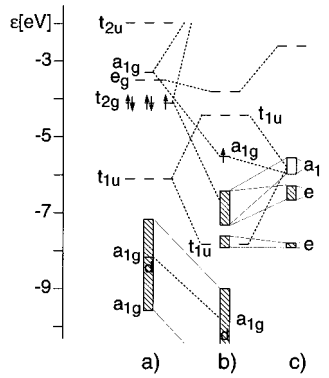

Figure 9. Orbital interaction diagram between Ag_{13} (a) and $[Fe(CO)_4]_8$ (c) to yield the $[Ag_{13}\{Fe(CO)_4\}_8]^{4-}$ cluster (b). Layout as in Figure 6.

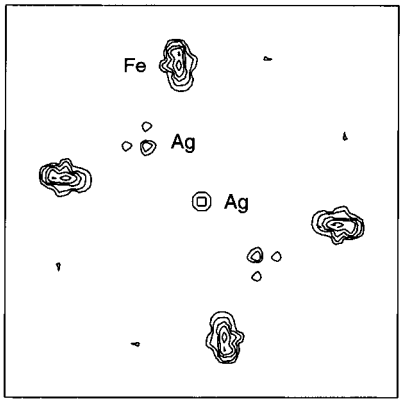

Figure 10. Calculated spin density $\Delta\rho = \rho^{\alpha} - \rho^{\beta}$ shown for a plane containing the central silver atom, two peripheral silver atoms, four iron atoms, and eight CO groups. The contour lines correspond to values of 0.002, 0.004, 0.008, 0.016, 0.031, and 0.063 au.

compound is a singly occupied e_u. In the cluster tetraanion, the singly occupied HOMO is of a_{1g} symmetry (Figure 9b).

For both the central and the outer silver atoms the 1s levels shift to higher binding energies by 1.67 and 1.90 eV, respectively, when the $Fe(CO)_4$ groups are added. In this cluster, too, the calculated core level shifts are in line with a charge transfer from the silver subsystem to the $Fe(CO)_4$ moieties.

The nature of the unpaired electron in the $[Ag_{13}\{Fe(CO)_4\}_8]^{4-}$ cluster has been studied by means of ESR spectroscopy.[6] The spin localized to about 25% on the central Ag atom and a negligible spin density on the peripheral Ag atoms means that the unpaired electron is significantly delocalized over the rest of the cluster, in particular over the $Fe(CO)_4$ groups. Unfortunately, the hyperfine coupling constant of the electron spin with the ^{57}Fe nuclear spin cannot be detected because of the low natural abundance of this isotope (2%) so that this information is not available from experiment. We have analyzed the distribution of the unpaired electron by means of a spin density map $\Delta\rho = \rho^{\alpha} - \rho^{\beta}$ in Figure 10. The calculation has been performed with integer occupation numbers so that the spatial integration of the density difference results in exactly one electron. The plot shows a considerable localization of the spin density on the Fe atoms, no spin density at all on the CO ligands, and a modest spin density on the central Ag atom and to a minor extent on the peripheral Ag atoms, in broad agreement with the interpretation of the ESR spectra.

5. Conclusions

LCGTO-DF calculations on a new class of bimetallic M_n-Fe_m carbonyl clusters (M = Cu, Ag, Au) allowed us to investigate the effect of the ligands on the cluster electronic structure, the periodic trends as one moves from Cu to Au, the optimal geometrical parameters, and the importance of relativistic effects.

The present study has shown that both conceivable classifications of this class of compounds, either as M−Fe bimetallic clusters stabilized by CO ligands or as coinage metal cores surrounded by $Fe(CO)_4$ moieties, are meaningful. The first assignment is supported by the strong ligand effect of the CO molecules, which leads to a substantial weakening of the metal−metal bonds in the M−Fe core and a quenching of the strong magnetism of the naked M_4Fe_4 clusters. It is important to stress that a planar rearrangement of the bare M_4Fe_4 metal core is not the favored one. For example, an Ag_4Fe_4 cluster formed by capping the faces of a Ag_4 tetrahedron with Fe atoms is calculated to be 1.4 eV more stable than the square-planar isomer. The second viewpoint demonstrates that the $Fe(CO)_4$ moieties can act as electron reservoirs. The interaction with the coinage metal core M_4 leads to a stabilization of the M d manifold and a destabilization of the M s orbitals, resulting in a charge transfer to the $Fe(CO)_4$ groups.

So far, the synthesis of the $[Cu_4\{Fe(CO)_4\}_4]^{4-}$ cluster has not been successful. It was suggested that this may be due to thermodynamic reasons.[1] The argument is based on the fact that an idealized tetrameric structure would require M−M contacts about 40% longer than M−Fe separations or an unfavorable deviation from a linear arrangement of the Fe−M−Fe units. In the optimized $[M_4\{Fe(CO)_4\}_4]^{4-}$ clusters, the M−M bond lengths are longer than the M−Fe bond distances by 14% for the Ag derivative and by 8% for the Cu compound. The calculations do not show a different stability of the $[Cu_4\{Fe(CO)_4\}_4]^{4-}$ anion with respect to the Ag and Au analogues. Thus, if the reason for the failure of the synthesis is of thermodynamic nature, this must be looked for in the relative stability of the molecular precursors (the reactants) and not in a lower stability of the product.

Calculations on the paramagnetic cluster anion $[Ag_{13}\{Fe(CO)_4\}_8]^{n-}$ ($n = 0-4$) and on the corresponding naked cluster $Ag_{13}Fe_8$ reveal similar features as for the tetramers. Addition of up to three electrons results in a stabilization of the cluster; this corresponds to the filling of the e_u cluster HOMO with a final closed-shell structure. The addition of the fourth electron into the a_{1g} orbital destabilizes the free cluster. This is not surprising given the large net charge (4−) and the Ag−Ag antibonding nature of the a_{1g} level. The tetraanion has been obtained in a crystalline form and characterized by ESR.[6] The calculated spin density shows a substantial localization of the unpaired electron on the Fe atoms and only a modest density on the central Ag atom. The analysis of the measured hyperfine coupling constants with the ^{107}Ag and ^{109}Ag isotopes has shown a 25% localization on the central Ag atom. Thus, it is likely that the rest of the spin population resides on the Fe atoms, in agreement with present results.

Acknowledgment. We thank M. Mayer for providing a tool for the fragment orbital analysis and V. A. Nasluzov for assistance during the geometry optimization. The work was supported by the European Human Capital and Mobility programme under Grant No. CHRX-CT 94 0532, by the Deutsche Forschungsgemeinschaft, and by the Fonds der Chemischen Instustrie.

IC960274G